

Grazing changes topography-controlled topsoil properties and their interaction on different spatial scales in a semi-arid grassland of Inner Mongolia, P.R. China

Angelika Kölbl · Markus Steffens · Martin Wiesmeier · Carsten Hoffmann · Roger Funk · Julia Krümmelbein · Agnieszka Reszkowska · Ying Zhao · Stephan Peth · Rainer Horn · Marcus Giese · Ingrid Kögel-Knabner

Received: 18 December 2009 / Accepted: 17 June 2010 / Published online: 3 July 2010
© Springer Science+Business Media B.V. 2010

Abstract Semiarid steppe ecosystems account for large terrestrial areas and are considered as large carbon (C) sinks. However, fundamental information on topsoil sensitivity to grazing is lacking across different spatial scales including the effects of topography. Our interdisciplinary approach considering soil chemical, physical, and vegetation properties included investigations on pit scale (square-metre scale), plot scale (hectare scale), and the scale of a landscape section (several hectares). Five different sites, representing a grazing intensity gradient, ranging from a long-term grazing enclosure to a heavily grazed site were used. On the pit scale, data about aggregate size distribution, quantity of different soil organic carbon (SOC) pools, SOC mineralisation,

hydraulic conductivity and shear strength was available for topsoil samples from representative soil profiles. Spatial variability of topographical parameters, topsoil texture, bulk density, SOC, water repellency, and vegetation cover was analysed on the basis of regular, orthogonal grids in differently grazed treatments by using two different grid sizes on the plot scale and landscape section. On the pit scale, intensive grazing clearly decreased soil aggregation and the amount of fresh, litter-like particulate organic matter (POM). The weak aggregation in combination with animal trampling led to an enhanced mineralisation of SOC, higher topsoil bulk densities, lower infiltration rates, and subsequently to a higher risk of soil erosion. On the plot scale, the effects of soil

Responsible Editor: Klaus Butterbach-Bahl.

A. Kölbl (✉) · M. Steffens · M. Wiesmeier ·
I. Kögel-Knabner
Lehrstuhl für Bodenkunde, Department of Ecology and
Ecosystem Sciences, Centre of Life and Food Sciences
Weihenstephan, Technische Universität München,
85350 Freising-Weihenstephan, Germany
e-mail: koelbl@wzw.tum.de

J. Krümmelbein
Chair of Soil Protection and Recultivation,
Brandenburg University of Technology,
Konrad-Wachsmann-Alle 6,
03046 Cottbus, Germany

A. Reszkowska · Y. Zhao · S. Peth · R. Horn
Institute of Plant Nutrition and Soil Science,
Christian-Albrechts-Universität zu Kiel,
Olshausenstrasse 40,
24118 Kiel, Germany

C. Hoffmann · R. Funk
Institute of Soil Landscape Research,
Leibniz-Centre for Agricultural Landscape Research (ZALF),
Eberswalder Str. 84,
15374 Müncheberg, Germany

M. Giese
Institute of Plant Production and Agroecology
of the Tropics and Subtropics, Universität Hohenheim,
Garbenstrasse 13,
70593 Stuttgart, Germany

structure disruption due to grazing are enhanced by the degradation of vegetation patches and resulted in a texture-controlled wettability of the soil surface. In contrast, topsoils of grazing exclosures were characterised by advantageous mechanical topsoil characteristics and SOC-controlled wettability due to higher POM contents. A combined geostatistical and General Linear Model approach identified topography as the fundamental factor creating the spatial distribution of texture fractions and related soil parameters on the scale of a landscape section. Grazing strongly interfered with the topography-controlled particle relocation processes in the landscape and showed strongest effects on the aboveground biomass production and biomass-related soil properties like SOC stocks. We conclude that interdisciplinary multi-scale analyses are essential (i) to differentiate between topography- and grazing-controlled spatial patterns of topsoil and vegetation properties, and (ii) to identify the main grazing-sensitive processes on small scales that are interacting with the spatial distribution and relocation processes on larger scales.

Keywords Steppe soils · Soil organic matter fractions · Organic carbon mineralisation · Wind erosion · Texture · Vegetation cover · Shear strength · Hydraulic conductivity · Water repellency · Anisotropy

Introduction

Increased grazing intensities in Northern Chinese grassland ecosystems lead to a serious reduction of plant biomass (Gao et al. 2009; Hoffmann et al. 2008b). This is often followed by the well documented problems of wind and water erosion and topsoil degradation in those regions (Cui et al. 2005; Dormaar and Willms 1998; Hoffmann et al. 2008b), which in turn intensify the deterioration of the vegetation. Many studies reported findings on individual degradation processes caused by overgrazing, but we are lacking integrated case studies that combine parameters related to soil, plant and topography.

Increasing grazing pressure changes chemical and physical topsoil properties, which may enhance soil degradation processes (Dormaar and Willms 1998; Krümmelbein et al. 2006; Krümmelbein 2007). Sheep trampling was found to be the main factor degrading topsoil structural properties by reducing water-stable

aggregation, infiltration rates, and increasing bulk density and penetration resistance (Proffitt et al. 1995; Steffens et al. 2008). Krümmelbein et al. (2006) reported an anisotropic saturated hydraulic conductivity with higher values in the horizontal compared to the vertical direction as a result of sheep trampling. This anisotropy, caused by structural degradation, was also mirrored by soil mechanical parameters such as increased precompression stress, platy structure, and an anisotropic water infiltration (Krümmelbein et al. 2008). Consequently, the enhanced runoff and the loss of soil material by wind erosion are actual risks to these sensitive ecosystems and demand a more site adjusted management.

Soil physical properties strongly depend on the soil organic carbon (SOC) content (Quiroga et al. 1998). In particular, organic matter affects aggregate stability with strong feedbacks to aggregate turnover and SOC dynamics (von Lützwow et al. 2006; Jastrow et al. 2007). Thus, maintenance of SOC is a key factor in the sustainability of grassland ecosystems (Conant et al. 2001). Grassland management strongly affects SOC stocks (Conant et al. 2001; Soussana et al. 2004), and associated soil properties. Wu et al. (2003) found that the soils of the semiarid to subhumid zone in northeast China, e.g. Phaeozems, are highly susceptible to SOC loss upon management change. Steffens et al. (2008) showed that SOC stocks of steppe topsoils deteriorated significantly following heavy grazing, remained stable if grazing was reduced or excluded for 5 years, and significantly recovered during 25 years of grazing exclusion. Beukes and Cowling (2003) showed in a shortgrass steppe that a short-duration, low-frequency, intensive grazing system resulted in a more active microbial community, increasing organic matter turnover rates and infiltration capacity. The SOC balance of these soils is maintained by root and shoot litter inputs which enter the soil as particulate organic matter (POM). Characterised by high turnover rates and great lability, POM functions as an indicator for high C input and SOC turnover rates in different land use systems (Buyanovsky et al. 1994; Kölbl et al. 2006, 2007; Noellemeier et al. 2006), especially in systems characterised by a perennial grass sward (Dubeux et al. 2006).

Topsoil properties may exhibit seasonal and spatial variability. For example, temporal changes in infiltration rates measured by Proffitt et al. (1995) were attributed to changes in drainage pore volume as a consequence of the growth and decay of plant roots, the formation

and disruption of a surface crust, and the processes of soil compaction and remoulding resulting from animal trampling. Cui et al. (2005) analysed the effect of grazing on the spatial variability of SOC. Compared to a grazing enclosure, the study showed no significant decrease of SOC content and no change of spatial heterogeneity of SOC under light grazing pressure for 20 years for Inner Mongolia grasslands. The authors ascribe this to compensatory growth effects, which may account for the relative stability of SOC contents in lightly grazed steppes. Zhao et al. (2007) found that increasing grazing intensity resulted in a more homogeneous spatial distribution of soil properties such as soil water contents (SWC), SOC content and water drop penetration times (WDPT), bulk densities (BD), and shear strength (SS), and ascribed this to soil compaction. Soil homogenisation was accompanied by a reduced input of organic matter and a reduced soil water storage capacity. Steffens et al. (2009a) explained the patchy and heterogeneous topsoil and vegetation properties found at ungrazed sites (compared to a homogeneous distribution at grazed sites) with increased deposition of windblown material interacting with vegetation succession dynamics.

Ungrazed sites were found to be well protected against wind erosion, and are characterised by high dust deposition and no losses through local dust emission (Hoffmann et al. 2008a). Thus, spatial homogenisation of vegetation and associated topsoil properties due to intensive grazing is a typical process of grassland degradation (Wiesmeier et al. 2009).

Since the mentioned studies report on single findings on different spatial scales, this article follows an interdisciplinary approach combining soil biochemical and physical processes, vegetation, and topography to analyse the effects of different grazing intensities from the pit to the landscape scale on topsoil properties of a steppe ecosystem. Therefore, the aims of the present case study were

- (i) to analyse the interrelationship between topsoil and vegetation parameters under different grazing intensities from the landscape section down to the pit scale
- (ii) to evaluate and differentiate between different grazing treatments and influences of topography (wind erosion) on topsoil and vegetation parameters

We hypothesised that grazing has a much higher impact on the interrelation and spatial distribution of

topsoil and vegetation properties than topographic features. A combined geostatistical and General Linear Model approach was applied to distinguish between grazing- and topography-related effects.

Materials and methods

Study area

The study area is situated in the vicinity of the Inner Mongolia Grassland Ecosystem Research Station (IMGERS, administered by the Chinese Academy of Sciences; 43°33' N, 116°40' E) in northeastern China, approximately 400 km north of Beijing near the city of Xilinhot (Fig. 1). The undulating landscape is characterised as a semiarid steppe ecosystem (*Stipa grandis*, *Leymus chinensis*). The altitude varies from 1,205 m to 1,285 m above sea level and the slopes have inclinations of <10° (Hoffmann et al. 2008a).

Climate is classified as a dry and cold middle latitude steppe climate. The mean annual temperature is 0.7°C. During the growing season between early May and late September, average monthly temperatures are above 5°C reaching a maximum of 19°C in July. The mean annual precipitation is 330 mm, with 85% occurring between May and September (Giese et al. 2009). Approximately 50 mm of the annual precipitation occurs as snow. Annual precipitation ranged from 166 to 325 mm during the investigated period (2004–2006; Giese et al. 2009). Almost all strong winds come regularly from northwest, separating windward and mostly sheltered leeward exposed slopes (Hoffmann et al. 2008a).

Plot description and soil classification

Measurements were conducted in five plots of different grazing intensities: two ungrazed plots fenced in 1979 and 1999 (UG79 (24 ha) and UG99 (25 ha)) and three plots with different grazing intensity. One plot is grazed only during wintertime (34 ha; winter grazing = WG), equivalent to a grazing intensity of 0.5 sheep units ha⁻¹ yr⁻¹ (1 sheep unit = 1 ewe and 1 lamb). Another plot (24 ha) is grazed during the whole year with the highest intensity during the summer months (continuously grazed = CG), equivalent to a grazing intensity of 1.2 sheep units ha⁻¹ yr⁻¹. The heavily

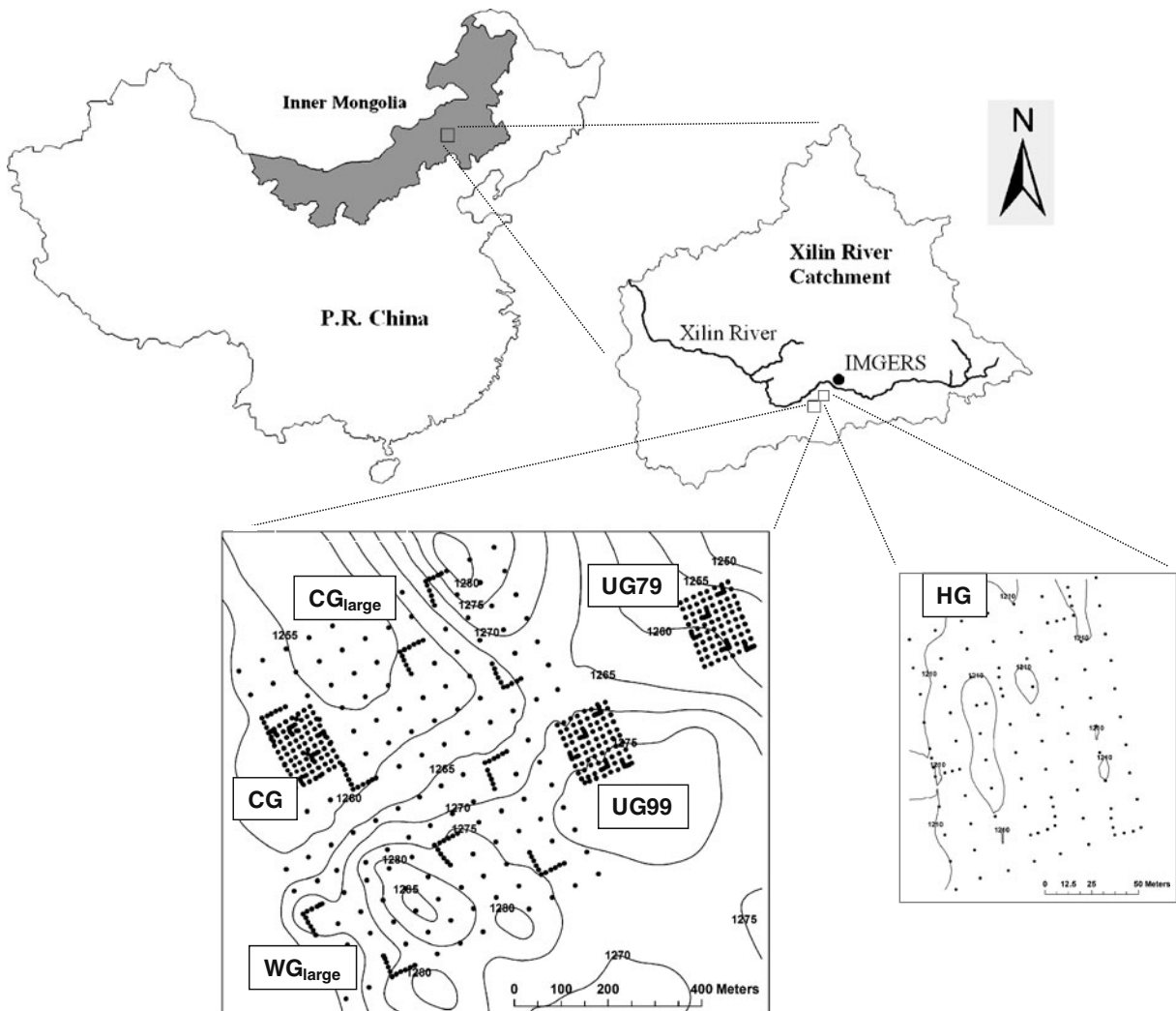


Fig. 1 Location of the experimental area in Northern China (IMGERS: Inner Mongolia Grassland Ecosystem Research Station), and location of the geostatistical areas on each plot.

Modified from Wiesmeier et al. (2009), Steffens et al. (2009a), and Zhao et al. (2007)

grazed plot is situated directly beside a farm and has been grazed continuously during the last 30 years (100 ha; heavily grazed = HG), representing a grazing intensity of 2.0 sheep units $\text{ha}^{-1} \text{yr}^{-1}$.

Soils are classified as Calcic Chernozems (IUSS Working Group WRB 2006) derived from aeolian sediments above acid volcanic rocks, which is the predominant soil type in the study area (Gong et al. 2008; Hoffmann et al. 2008a). The substrates are loam and sandy loam with more than 50% of fine sand and silt, which indicates the strong contribution of aeolian deposits to the formation of these soils (Hoffmann et al. 2008a). Depending on topography,

the thickness of the Ah horizon varies from 20–30 cm at hilltops to >100 cm at sheltered depressions and shallow leeward slopes. Carbonates were found in soil depths deeper than approx. 30 cm (decalcification of the upper 30 cm and/or lime precipitation due to capillary rise effects in the dry steppe climate). Topsoil pH values range between 6.8 and 7.1 and are comparable between differently grazed plots. Radiocarbon dating of topsoil organic matter shows pMC (percent modern carbon) values between 105 (CG) and 112 (UG79) in the 0–10 cm layer (Ah1), corresponding to a radiocarbon age younger than 1954 in all plots (Steffens et al. 2009b).

Sampling design and analyses of soil properties

Topsoil characteristics—derived from soil profile analyses

Three representative soil profiles were sampled at each plot. In this study, we summarised results from Krümmelbein et al. (2006) and Steffens et al. (2009b) and focus on the results of the upper soil layer (0–10 cm, Ah1).

Bulk soil material was sieved to three different aggregate size classes (6.3–2.0 mm, 2.0–0.63 mm, and <0.63 mm), showing only 17–25% in particles and aggregates >630 μm (Table 1; data from Steffens et al. 2009b). This low macroaggregation was accompanied by a loamy to sandy texture, with sand contributing between 45 and 64%, silt between 18 and 29%, and clay between 18 and 27%. HG is spatially separated from the other plots (Fig. 1) and is characterised by highest sand and lowest clay contents. All other plots showed comparable textures and states of macroaggregation.

Undisturbed soil samples were taken at 4–8 cm depth for analyses of soil physical parameters (precompression stresses, shear parameters, and hydraulic conductivity; Krümmelbein et al. 2006). Although there were no statistically significant differences, there were some obvious trends between grazed and ungrazed sites. The angle of internal friction describes the degree of aggregation and was a little lower in grazed topsoils ($\phi=34\text{--}37^\circ$) than in ungrazed topsoils ($\phi=37\text{--}40^\circ$; Table 1; data from Krümmelbein et al. 2006). Slightly higher cohesion values of grazed plots (26–30 kPa) compared to ungrazed plots (15–19 kPa) reflected the more compressed situation of the grazed topsoil. Due to the loamy to sandy texture of the soils, the saturated hydraulic conductivity (K) of the different treatments was relatively high, with mean values between 46 and 165 cm d^{-1} . The mean values decreased with increasing grazing intensity in the order UG79 > UG99 > HG > WG. The slightly higher mean value of the heavily grazed plot was ascribed to the slightly higher sand content of this plot. Beside the mean values, much higher standard deviations of the ungrazed compared to the grazed plots denoted a higher variability of K due to the higher degree of aggregation.

Disturbed bulk soil samples were subjected to a physical fractionation procedure to obtain specific soil fractions. The free particulate organic matter (fPOM) was separated by density fractionation using a Na-

polytungstate solution ($\rho=1.8 \text{ g cm}^{-3}$). To obtain the POM occluded in aggregates (oPOM), the residual heavy fraction ($>1.8 \text{ g cm}^{-3}$) was treated by ultrasound, using an energy input of 150 J ml^{-1} (treatment times were adjusted to sample volume, approximately 10 min) to disrupt all macroaggregates. With a subsequent density fractionation step (Na-polytungstate solution, $\rho=1.8 \text{ g cm}^{-3}$), the oPOM floating on the suspension was obtained after centrifugation (Steffens et al. 2009b). The fractions were washed with bidistilled water, freeze-dried, weighed, and ground for further analyses. Total C and total N concentrations of bulk soil and soil fractions were determined on a Vario EL elemental analyser (Elementar Analysensysteme GmbH, Hanau). Since all samples of the upper 10 cm were free of carbonate, the total C concentration equals the soil organic carbon (SOC) concentration. SOC concentrations of the bulk soil ranged between 21.3 and 22.8 mg g^{-1} in UG79, UG99 and WG, and were tendentially lower in CG and HG (16.7 and 16.5 mg g^{-1} , respectively) (Table 1). Total N concentrations showed a comparable trend. The resulting C/N ratios vary between 9.1 and 10.5, regardless of grazing intensity. The mass of the fPOM was much higher in UG79 than in all other treatments, and contributed 35% to the total SOC content in this plot (Table 1). The oPOM showed lower contents throughout all treatments compared to the fPOM. The content of oPOM was higher in both ungrazed plots compared to the grazed plots. The contribution of oPOM to total SOC was 13% and 15% in UG79 and UG99, compared to 7% in WG and CG. Total POM contents of the sandier HG plot were higher compared to the other grazed plots.

Carbon mineralisation of bulk samples was determined for a period of one month at a constant temperature of 20°C with an automated incubation system according to Heinemeyer et al. (1989) which was improved according to Müller (2009). The calculated release of $\text{CO}_2\text{-C}$ was related to the SOC content of the soil samples. Carbon mineralisation ranged between 8.0 and 9.0 $\text{mg CO}_2\text{-C g}^{-1} \text{ SOC}$ for UG79, UG99 and WG (Table 1). For CG and HG, significantly higher releases of 12.8 and 17.0 $\text{mg CO}_2\text{-C g}^{-1} \text{ SOC}$ were determined.

Grid sampling

On each plot, a regular, orthogonal sampling grid was set up (Fig. 1). On CG and WG large grids (300 m \times

Table 1 Physical and chemical properties derived from soil profiles (0–10 cm, upper layer of Ah) given as arithmetic means (**bold**) and standard deviations of three soil pits

			UG79	UG99	WG	CG	HG
ASD ^a	6.3–2.0 mm	[%]	7	10	14	11	11
	2.0–0.63 mm	[%]	10	11	11	9	6
	<0.63 mm	[%]	83	79	75	80	83
Texture ^a	Sand	[mg g ⁻¹]	600	450	500	560	640
			41	40	40	80	30
	Silt	[mg g ⁻¹]	180	290	230	200	180
			40	40	40	50	20
Shear strength ^b	Clay	[mg g ⁻¹]	220	260	270	240	180
			10	0	10	30	10
	ϕ	[°]	37.6	39.8	34.0	–	36.8
Hydr. conduct. ^b	C	[kPa]	14.6	18.8	25.9	–	29.8
			3.9	6.6	11.0	–	9.3
	K	[cm d ⁻¹]	165	132	46	–	99
Organic matter ^a	SOC	[mg g ⁻¹]	21.3	22.8	21.5	16.7	16.5
			1.8	3.0	3.0	3.8	–
	N	[mg g ⁻¹]	2.06	2.34	2.18	1.84	1.57
			0.1	0.27	0.21	0.46	–
^a	C/N		10.3	9.7	9.9	9.1	10.5
	fPOM	weight [mg (g soil) ⁻¹]	31.6	15.2	12.6	16.4	25.0
		fPOM-OC [mg (g soil) ⁻¹]	7.1	2.8	1.7	2.4	4.4
^a	fPOM-OC	[mg (g SOC) ⁻¹]	355	127	95	123	265
	oPOM	weight [mg (g soil) ⁻¹]	8.4	11.9	5.8	5.7	7.7
		oPOM-OC [mg (g soil) ⁻¹]	2.6	3.3	1.5	1.6	2.1
SOC min.	oPOM-OC	[mg (g SOC) ⁻¹]	134	155	73	74	127
	CO₂-C	mg g ⁻¹ SOC	7.97	9.02	8.97	12.76	16.98
			0.52	0.30	0.60	0.53	0.89

ASD: aggregate size distribution after dry sieving of topsoil material. ϕ : Angle of internal friction. C: Cohesion. Hydr. conduct.: saturated hydraulic conductivity. SOC: Soil organic carbon. fPOM: free particulate organic matter. oPOM: occluded particulate organic matter. SOC min.: SOC mineralization. HG: heavily grazed, CG = continuously grazed, WG = winter grazing, UG99 = ungrazed since 1999, UG79 = ungrazed since 1979

^a Data from Steffens et al. 2009b, modified

^b Data from Krümmelbein et al. 2006, modified

550 m; further denominated as CG_{large} and WG_{large}) and on HG, CG, UG99 and UG79 small grids (105 m × 135 m) were sampled. Both large grids consisted of 125 sampling points with a spacing of 50 m, the four small grids contained 100 sampling points each with 15 m spacing. Small-scale variability was considered through additional sampling nests with spacing of 10 m and 5 m within large and small grids, respectively (Steffens et al. 2009a). The altitude

was measured at every sampling point in UG79, UG99, CG, WG_{large} and CG_{large} using a Real Time Kinematic Differential GPS. A digital terrain model and topographical features as aspect, slope, and curvature were derived by Arc INFO topogrid (ESRI® 2006, Germany; Hoffmann et al. 2008a).

Thickness of Ah was determined with a soil auger at every other sampling position and when topography changed at every position (387 points). At each

sampling point, the upper 4 cm of soil were sampled in triplicate with a stainless steel cylinder (100 cm³) and bulked to obtain a composite sample (resulting in a total sample number of 650 as described in Steffens et al. 2009a). Each soil sample was analysed for bulk density (BD), total C, and total N concentration, and pH (650 points). BD of the soil was calculated with the mass of the oven-dry soil (105°C) divided by the core volume (Hartge and Horn 2009). Prior to chemical analyses, samples were sieved to <2 mm. Total C and total N concentrations were determined in duplicate by dry combustion on a Vario Max CNS elemental analyser (Elementar Analysensysteme GmbH, Hanau, Germany). As described in Steffens et al. (2008), SOC and N stocks of the upper 4 cm were calculated using an equivalent mass instead of BD to consider changes in BD following grazing (Ellert and Bettany 1995; Veldkamp 1994). Soil pH was determined in a 1:2.5 soil to 0.01 M CaCl₂ solution. Soil texture was measured by sieving and pipette method, as summarised in Hoffmann et al. (2008b) and Zhao et al. (2007). At each grid point of the small grids, water repellency was measured using the WDPT test, where the elapsed time was recorded for a droplet of distilled water (0.5 mm³, using a standard glass pipette) to completely infiltrate into the smoothed soil surface. Shear strength (SS) was measured by a portable shear vane tester (Geonor H-60, Norway). Hydraulic conductivity (K) was measured with a Mini-disk Infiltrometer (Decagon devices, USA) at a suction of 2 hPa (Zhao et al. 2007). Vegetation cover and plant species composition were obtained from 1 m² subplots at 550 sampling points (UG79, UG99, HG, WG_{large} and CG_{large}), using a non-destructive visual sampling method based on cover-abundance classes. Aboveground biomass was harvested at peak time (August 2004) at all sampling points by cutting a 0.25 m×0.25 m square at 1 cm height.

Statistical and geostatistical analysis

Descriptive statistical analyses were carried out using SPSS 17.0 (SPSS Inc., Chicago, USA). Interrelationships between topsoil and vegetation parameters were analysed by correlation analyses, calculating Spearman's rank correlation coefficients (Sigma Plot 11.0, Systat Software Inc., San Jose, California, USA). The spatial behaviour of selected topsoil properties in differently grazed plots was investigated using geostatistical analy-

ses with R 2.8.0 (RDevelopmentCoreTeam 2008) in combination with the g-stat 2.8.0 package (Pebesma 2004). Prior to geostatistical analysis each parameter in each plot was tested for normal distribution using the Kolmogoroff-Smirnoff-Test. The nugget-to-sill ratio (Nu/Si) was calculated from semivariograms (referred to as Co/Co+C_s) as an indicator for the degree of spatial dependence. Low ratios point towards a low relative nugget effect and lead to the assumption of a stronger spatial dependency (Cambardella et al. 1994). Large range values support the assumption of a more homogeneous spatial distribution of the analysed parameter. Large Nu/Si ratios accompanied by small range values indicate that a large portion of the variance takes place at small scales. This shows a more heterogeneous, patchy distribution and leads to the assumption that small-scale processes control the spatial distribution of this parameter. In order to display the spatial distribution of selected topsoil properties, thematic maps were created with an ordinary kriging procedure (Arc Map 9.2, ESRI® 2006, Germany) using the semi-variogram parameters obtained with g-stat.

SPSS 17.0 (SPSS Inc., Chicago, USA) was used to classify topography data (altitude, aspect, slope, and curvature) applying a two-step cluster analysis procedure. To differentiate between these topographical factors and grazing effects on selected topsoil and vegetation variables, General Linear Model (GLM) procedures with a full factorial design and least significant difference (LSD) tests as post-hoc tests were used. In this context, two GLM procedures were applied, one considering topographical features alone and a second approach, including grazing treatments as additional influencing factor. This approach was applied to WG_{large}, CG_{large}, CG, UG99 and UG79. HG was situated too distant to the other areas (Fig. 1) and was therefore excluded from investigations needing a contiguous landscape section.

Results

Topsoil characteristics derived from grid sampling and analyses

All grids samples had a loamy texture (mean values of sand: 44–51%, silt: 32–38%, clay: 16–18%; Tables 2 and 3). HG showed higher sand contents

Table 2 Descriptive statistics of physical and chemical topsoil parameters (small grids, 0–4 cm) during the period of 2004–2006

Parameters		Mean	SD	<i>n</i>		Mean	SD	<i>n</i>		
HG	Coarse sand [mg g ⁻¹]	4	b	2	100	UG 79	12	a	5	55
	Medium sand [mg g ⁻¹]	134	a	24	100		146	a	41	55
	Fine sand [mg g ⁻¹]	543	a	31	100		338	d	25	55
	Coarse silt [mg g ⁻¹]	138	d	19	100		213	b	31	55
	Medium silt [mg g ⁻¹]	45	c	11	100		90	a	15	55
	Fine silt [mg g ⁻¹]	26	b	6	100		43	a	7	55
	Clay [mg g ⁻¹]	110	b	19	100		159	a	18	55
	BD ^a [g cm ⁻³]	1.28	a	0.08	98		0.94	d	0.10	98
	SS [kPa]	56.4	ab	12.9	98		59.1	a	8.2	98
	WDPT [s]	1.9	c	1.2	98		21.6	a	19.2	98
	K [cm d ⁻¹]	51.1	a	11.9	98		26.1	c	12.9	98
	SOC ^a [mg g ⁻¹]	17.0	d	4.2	98		31.0	a	5.5	98
	N ^a [mg g ⁻¹]	1.74	d	0.39	98		3.14	a	0.50	98
	SOC stocks ^a [kg m ⁻²]	0.64	d	0.16	98		1.17	a	0.20	98
	N stocks ^a [kg m ⁻²]	0.07	d	0.02	98		0.12	a	0.02	98
	C/N ^a	9.7	a	0.4	98		9.8	a	0.3	98
	pH ^a	6.6	b	0.2	97		6.6	b	0.2	98
	Ah [cm]	104	a	2	78		86	c	10	47
	Cover [%]	70	b	12	98		76	a	9	98
	Biomass [g m ⁻²]	132	c	42	97		311	b	77	98
Species No.	11.8	b	2.1	74	18.4	a	3.5	76		
CG	Coarse sand [mg g ⁻¹]	2	c	0	88	UG 99	12	a	6	50
	Medium sand [mg g ⁻¹]	76	c	16	88		99	b	21	50
	Fine sand [mg g ⁻¹]	433	b	39	88		359	c	55	50
	Coarse silt [mg g ⁻¹]	201	c	20	88		238	a	22	50
	Medium silt [mg g ⁻¹]	76	b	11	88		86	a	19	50
	Fine silt [mg g ⁻¹]	44	a	7	88		44	a	10	50
	Clay [mg g ⁻¹]	168	a	21	88		163	a	22	50
	BD ^a [g cm ⁻³]	1.21	b	0.07	88		1.09	c	0.12	99
	SS [kPa]	54.1	b	9.70	88		59.2	a	7.27	99
	WDPT [s]	5.8	c	2.7	88		15.6	b	14.9	99
	K [cm d ⁻¹]	43.0	b	11.2	88		54.8	a	14.8	99
	SOC ^a [mg g ⁻¹]	22.2	c	3.7	88		25.5	b	6.3	99
	N ^a [mg g ⁻¹]	2.36	c	0.40	88		2.65	b	0.67	99
	SOC stocks ^a [kg m ⁻²]	0.84	c	0.14	88		0.96	b	0.24	99
	N stocks ^a [kg m ⁻²]	0.09	c	0.02	88		0.10	b	0.03	99
	C/N ^a	9.4	b	0.4	88		9.7	a	0.7	99
	pH ^a	6.8	a	0.4	86		6.8	a	0.3	99
	Ah [cm]	98	b	7	69		77	d	15	52
	Cover [%]	–	–	–	–		68	b	8	99
	Biomass [g m ⁻²]	–	–	–	–		405	a	70	99
Species No.	–	–	–	–	8.9	c	1.5	77		

^aData from Steffens et al. 2008

BD: bulk density; K: saturated hydraulic conductivity; WDPT: water drop penetration time; SS: shear strength. SOC: soil organic carbon concentration; N: total nitrogen concentration, SOC and N stocks calculated according to equivalent mass approach (Steffens et al. 2008). SD: Standard deviation; n: number of analysed grid points. Different letters indicate significantly different mean values between grazing intensities ($p < 0.01$)

Table 3 Descriptive statistics of physical and chemical topsoil parameters (large grids, 0–4 cm)

Parameters		Mean	SD	<i>n</i>	Mean	SD	<i>n</i>			
WG _{large}	Coarse sand [mg g ⁻¹]	18	a	18	70	CG _{large}	19	a	25	88
	Medium sand [mg g ⁻¹]	86	a	25	70		98	a	34	88
	Fine sand [mg g ⁻¹]	337	b	46	70		377	a	41	88
	Coarse silt [mg g ⁻¹]	230	a	27	70		208	b	28	88
	Medium silt [mg g ⁻¹]	99	a	17	70		83	b	15	88
	Fine silt [mg g ⁻¹]	48	a	9	70		43	b	8	88
	Clay [mg g ⁻¹]	182	a	19	70		171	b	21	88
	BD [g cm ⁻³] ^a	1.09	b	0.08	122		1.17	a	0.07	123
	SOC [mg g ⁻¹] ^a	25.9	a	4.48	122		23.0	b	4.13	123
	N [mg g ⁻¹] ^a	2.72	a	0.44	122		2.40	b	0.40	123
	SOC stocks [kg m ⁻²] ^a	0.98	a	0.17	122		0.87	b	0.16	123
	N stocks [kg m ⁻²] ^a	0.10	a	0.02	122		0.09	b	0.02	123
	C/N ^a	9.5	a	0.4	122		9.6	a	0.4	123
	pH ^a	6.7	a	0.3	122		6.6	b	0.4	123
	Altitude [m a.s.l.]	1,273	a	5	122		1,261	b	6	123
	Aspect [°]	221	a	119	122		217	a	98	123
	Slope [%]	7.3	a	3.4	122		6.1	a	4.5	123
Plant cover [%]	60	a	13	118	56	a	16	103		
Aboveground biomass [g m ⁻²]	167	a	39	122	163	a	68	113		
Ah [m]	64	b	21	72	82	a	21	68		

^aData from Steffens et al. 2008

BD: bulk density; SOC: soil organic carbon concentration; N: total nitrogen concentration, SOC and N stocks calculated according to equivalent mass approach (Steffens et al. 2008). Different letters indicate significantly different mean values between grazing intensities ($p < 0.01$)

(68%), and lower silt (21%) and clay contents (11%). This is mainly due to the significantly higher proportion of fine sand in this area.

Within the small grids (Table 2), topsoil BD increased with increasing grazing intensity, with mean values ranging from 0.94 g cm⁻³ at UG79 to 1.28 g cm⁻³ at HG. SOC concentrations of the topsoils strongly decreased with increasing grazing intensity from 31 mg g⁻¹ at UG79 to 17 mg g⁻¹ at the HG plot. N concentrations decreased in the same order from 3.1 to 1.7 mg g⁻¹. The resulting SOC and N stocks also significantly decreased with increasing grazing intensity. The C/N ratios ranged from 9.4 to 9.8 and the pH values between 6.6 and 6.8. Both parameters showed no discernible trend between grazing intensities (Table 2).

In contrast to the laboratory measurements (Table 1), SS measurements in the field were generally higher, with slightly higher values at ungrazed sites (59 kPa) compared to grazed sites (54–56 kPa). K values ranged between 26 and 55 cm d⁻¹, without a clear trend

between grazing intensities. However, WDPT was significantly higher in ungrazed than in grazed plots, and decreased with increasing grazing intensity (Table 2).

Mean values and ranges of topsoil parameters measured at CG_{large} (Table 3) showed comparable values to those obtained from the small grid of CG (Table 2). This indicates that reliable mean values to characterise topsoil properties of the different grazing intensities can be obtained by both grid sizes. Similarly to the small grids, the mean values of large grids also showed a higher BD, but lower SOC and N concentrations for the higher grazing intensity, resulting in significantly lower SOC and N stocks at the CG plot (Table 3). Additionally collected data concerning the vegetation cover of the larger scale showed no significantly different values between the two sites.

In addition to the comparison of mean values, correlation matrices were calculated for all variables (Table 4a–d; Table 5a–b). SS, aboveground biomass and

Table 4 Correlation matrix of soil, vegetation and topographic parameters – small grids

	K	BD	SOC	N	pH	Ah	Cover	Altitude	Slope	cS	mS	fS	cSi	mSi	fSi	CI	Spec. No	C4/C3
a: UG79																		
WDPT	-0.36***	-0.37***	0.38***	0.40***	-0.34***	0.08	0.09	0.19	-0.15	-0.24	-0.30	-0.14	0.20	0.29	0.22	0.24	-0.41***	0.12
K		0.34***	-0.36***	-0.37***	0.30**	-0.08	-0.15	-0.35***	0.28**	0.22	0.11	0.07	0.03	-0.16	-0.26	-0.16	0.31**	-0.07
BD			-0.89***	-0.88***	0.39***	-0.47***	-0.16	0.07	-0.09	0.53***	0.61***	0.22	-0.37*	-0.67***	-0.25	-0.55***	0.17	-0.02
SOC				0.99***	-0.40***	0.44**	0.19	-0.05	0.09	-0.54***	-0.62***	-0.23	0.36*	0.60***	0.35*	0.55***	-0.18	-0.01
N					-0.44***	0.36*	0.17	-0.01	0.07	-0.52***	-0.59***	-0.20	0.34*	0.60***	0.33*	0.50***	-0.23*	0.01
pH						-0.02	-0.24*	-0.16	0.23*	0.25	0.23	0.06	-0.10	-0.18	-0.36*	-0.13	0.18	-0.08
Ah							0.38**	-0.55***	0.57***	-0.36	-0.89***	-0.41	0.88***	0.50*	0.07	0.86***	0.16	-0.22
Cover								-0.15	0.11	-0.06	-0.11	-0.02	0.15	0.02	0.11	0.02	0.12	-0.19
Altitude									-0.85***	0.21	0.46**	0.11	-0.47**	-0.20	-0.19	-0.31*	-0.41***	0.11
Slope										-0.24	-0.44**	-0.01	0.44**	0.16	-0.06	0.32*	0.35**	-0.10
cS											0.59***	-0.10	-0.40**	-0.28	-0.18	-0.41**	0.53**	0.08
mS												0.31*	-0.82***	-0.58***	-0.43**	-0.76***	0.16	0.22
fS													-0.54***	-0.51***	-0.35*	-0.51***	-0.20	0.09
cSi														0.33*	0.28	0.54***	-0.03	-0.20
mSi															0.42**	0.68***	-0.09	-0.08
fSi																0.25	-0.07	-0.02
CI																	-0.14	-0.15
Spec. No																		-0.02
b: UG99																		
WDPT	-0.15	-0.27**	0.28**	0.27**	-0.14	-0.40**	-0.37***	0.00	-0.13	0.44**	0.03	-0.40**	0.08	0.43**	0.41**	0.24	-0.28*	0.16
K		0.10	-0.15	-0.14	0.04	0.11	0.04	0.15	0.10	-0.13	0.10	0.07	-0.35*	0.07	-0.12	0.11	-0.03	0.10
BD			-0.92***	-0.91***	0.59***	-0.12	0.06	-0.01	-0.27**	-0.57***	0.19	0.78***	-0.34*	-0.69***	-0.75***	-0.64***	0.22	0.18
SOC				0.99***	-0.65***	0.04	-0.08	0.14	0.20*	0.73***	-0.13	-0.88***	0.42**	0.69***	0.80***	0.68***	-0.24*	-0.19
N							-0.08	0.16	0.22*	0.74***	-0.16	-0.90***	0.45**	0.70***	0.82***	0.69***	-0.24*	-0.18
pH							0.05	-0.04	-0.15	-0.51***	0.15	0.70***	-0.33*	-0.58***	-0.60***	-0.68***	0.19	0.15
Ah								-0.11	0.38**	-0.43	-0.24	0.44	-0.30	-0.21	-0.20	0.04	0.24	-0.35*
Cover								0.005	0.14	-0.14	0.19	0.14	-0.03	-0.22	-0.16	-0.05	0.32**	-0.18
Altitude									-0.35***	0.24	0.38*	-0.25	-0.21	0.17	0.19	0.21	-0.09	0.12
Slope										0.11	-0.27	-0.24	0.15	0.22	0.16	0.39*	-0.12	-0.32**
cS											0.17	-0.72***	0.22	0.41**	0.74***	0.45**	-0.33	0.16
mS												0.20	-0.69***	-0.35*	-0.23	-0.27	0.17	0.16
fS													-0.50***	-0.81***	-0.85***	-0.85***	0.54**	-0.04
cSi														0.33*	0.40**	0.36*	-0.31	0.02

mSi	0.67***	0.75***	-0.48**	0.00
fSi	0.63***	-0.41*	0.06	
Cl		-0.41*	-0.05	
Spec. No		0.15		
c: CG				
WDPT	0.02	0.11	-0.03	-0.09
K	0.02	0.01	0.04	0.22*
BD		0.46***	0.18	0.61***
SOC		-0.39***	-0.13	-0.66***
N		-0.38***	-0.09	-0.57***
pH		0.33**	0.15	0.05
Ah		-0.34**	0.09	-0.06
Cover		n.d.	n.d.	n.d.
Altitude		0.09	0.25*	0.00
Slope		0.21	0.38***	0.46***
cS		0.20	0.37***	0.20
mS		0.77***	-0.79***	-0.79***
fS		-0.83***	-0.81***	-0.83***
cSi		0.64***	0.72***	0.62***
mSi		0.68***	0.61***	0.68***
fSi		0.65***	0.61***	0.65***
Cl		n.d.	n.d.	n.d.
Spec. No		n.d.	n.d.	n.d.
d: HG				
WDPT	-0.18	0.30**	-0.48***	-0.48***
K	-0.12	0.18	0.21*	-0.82***
BD		-0.79***	-0.35***	0.03
SOC		0.99***	0.45***	-0.14
N		0.47***	-0.15	0.08
pH		0.08	0.08	0.08
Ah		-0.05	-0.05	-0.05
Cover		n.d.	n.d.	n.d.
Altitude		0.64***	0.04	0.64***
Slope		n.d.	n.d.	n.d.
cS		0.54***	0.54***	0.54***
mS		-0.80***	-0.80***	-0.80***

Table 4 (continued)

	K	BD	SOC	N	pH	Ah	Cover	Altitude	Slope	cS	mS	fS	cSi	mSi	fSi	Cl	Spec. No	C4/C3
fS													-0.68***	-0.82***	-0.74***	-0.81***	-0.34**	0.25*
cSi														0.70***	0.67***	0.69***	0.53***	-0.29*
mSi															0.80***	0.82***	0.27*	-0.29*
fSi																0.75***	0.36**	-0.25*
Cl																	0.36**	-0.19
Spec. No																		0.04

WDPT: water drop penetration time; K: saturated hydraulic conductivity; BD: bulk density; SOC: soil organic carbon concentration; N: total nitrogen concentration; Ah: thickness of Ah horizon; cS: coarse sand; mS: medium sand; fS: fine sand; cSi: coarse silt; mSi: medium silt; fSi: fine silt; Cl: clay; Spec.No.: Number of plant species; C4/C3: proportion of C₄-to-C₃ plants

Level of significance: *: $p \leq 0.05$; **: $p \leq 0.01$; ***: $p \leq 0.001$

the topographical parameters aspect and curvature are not correlated with any other parameter within the individual plots. These parameters were excluded from further correlation analyses in the small grids but were still considered in the large grids. The fine texture fractions (silt and clay) correlated highly significant with BD, SOC and N. In both ungrazed plots (Table 4a-b), WDPT showed positive correlations with SOC and N, but negative correlations with BD. K showed only in UG79 significant correlations with BD, SOC and N. In HG, WDPT showed correlations with BD, SOC and N in the opposite direction as compared to ungrazed plots. Additionally, WDPT and K correlated highly significantly with texture (Table 4d). Within small grids, topographical features mainly influenced Ah values, with negative correlations between Ah and altitude, and positive correlations between Ah and slope.

Both ungrazed plots additionally showed positive correlations between vegetation cover and thickness of Ah. Other vegetation parameters (number of species, proportion of C₄-to-C₃ plants) as well as topographical parameters (altitude and slope) showed only weak correlations, without an identifiable trend between different parameters and grazing intensities.

Within large grids (Table 5), texture showed also highly significant correlations with BD, SOC and total N. In CG_{large}, topographical parameters (altitude and slope) showed strong correlation with all texture fractions, with positive correlations in coarse and medium sand and negative correlations in finer particle size fractions. The same trend was found in WG_{large} with lower significance, indicating a sorting of particle size fractions in the landscape. In CG_{large}, negative correlations between topographical parameters (altitude and slope) and Ah thickness, vegetation cover and aboveground biomass were observed. This negative relation was less pronounced in WG_{large}. At both plots, the negative relationship between altitude and vegetation cover was accompanied by highly significant positive correlations between altitude and the ratio of C₄-to-C₃ plants (i.e. a higher contribution of C₄ plants at higher landscape positions).

Spatial variability of topsoil properties

Within small grids, SOC and BD of UG79 showed relatively large Nu/Si values of 0.46 and 0.54, accompanied with small range values of ≤ 60 m (Table 6). All other small grids had lower Nu/Si

Table 5 Correlation matrix of soil, vegetation and topographic parameters – large grids

	SOC	N	pH	Ah	Cover	Bio-mass	Altitude	Aspect	Slope	Curv.	cS	mS	fS	eSi	mSi	fSi	CI	C3_cov	C4_cov	Spec. No	C4/C3
a: WC_{large}																					
BD	-0.79***	-0.80***	0.34***	0.12	-0.13	-0.12	-0.06	-0.15	-0.26**	-0.19*	0.23	0.55***	0.52***	-0.45***	-0.67***	-0.49***	-0.58***	-0.22*	0.33***	0.23*	0.32***
SOC		0.98***	-0.37***	-0.19	0.09	0.13	0.17	0.07	0.11	0.08	-0.13	-0.40**	-0.48***	0.44***	0.55***	0.34**	0.50***	0.11	-0.28**	-0.24**	-0.25**
N			-0.41***	-0.25*	0.04	0.10	0.22*	0.04	0.12	0.14	-0.09	-0.39**	-0.52***	0.45***	0.59***	0.35**	0.50***	0.07	-0.26**	-0.27**	-0.22*
pH				0.28*	0.00	0.01	-0.32***	-0.11	-0.12	-0.12	-0.39**	-0.14	0.33*	0.15	-0.33*	-0.23	-0.08	0.05	-0.08	0.05	-0.08
Ah					0.07	0.15	-0.39***	0.03	-0.04	-0.41***	-0.39*	-0.08	0.43**	0.12	-0.31	-0.33*	-0.25	0.07	-0.08	0.00	-0.11
Cover						0.22*	-0.13	0.10	-0.01	-0.17	-0.19	-0.26	-0.01	0.01	0.13	0.07	0.19	0.70***	-0.05	-0.01	-0.26**
Biomass							-0.20*	0.19*	-0.05	-0.18*	-0.18	-0.35**	0.04	0.18	-0.03	0.17	0.09	0.28**	-0.22*	0.10	-0.24**
Altitude								-0.37***	0.05	0.18*	0.75***	0.43***	-0.46***	-0.23	0.17	0.02	-0.08	-0.31***	0.26**	-0.18*	0.28**
Aspect									0.20*	-0.04	-0.37**	-0.21	0.23	0.06	-0.09	0.07	0.11	0.23	-0.24**	-0.04	-0.26**
Slope										0.28**	0.23	-0.39**	-0.37**	0.43***	0.25	0.39	0.03	0.02	-0.11	0.05	-0.08
Curv.											0.15	-0.04	-0.29*	-0.01	0.26*	0.09	0.13	-0.13	0.06	-0.10	0.10
cS												0.45***	-0.36**	-0.30*	0.07	0.03	-0.22	-0.34*	0.27*	0.16	0.31*
mS													0.23	-0.71***	-0.45***	-0.48***	-0.59***	-0.57***	0.60***	0.29*	0.64***
fS														-0.36**	-0.76***	-0.59***	-0.52***	-0.11	0.25	0.30*	0.22
eSi															0.26	0.39**	0.25	0.22	-0.48***	-0.29*	-0.46***
mSi																0.54***	0.60***	0.33*	-0.36**	-0.37**	-0.35**
fSi																	0.34**	0.33*	-0.40**	-0.25	-0.39**
CI																		0.36**	-0.37**	-0.24	-0.38**
C3_cov																			-0.57***	0.04	-0.75***
C4_cov																				0.08	0.96***
Spec. No																					0.07
b: CG_{large}																					
BD	-0.84***	-0.83***	0.19*	-0.44***	-0.26**	-0.03	0.24**	-0.17	0.23*	0.17	0.21	0.54***	0.45***	-0.41***	-0.70***	-0.62***	-0.70***	-0.31**	0.16	0.04	0.33***
SOC		0.97***	-0.13	0.29*	0.24*	0.06	-0.18	0.16	-0.22*	-0.17	-0.28*	-0.51***	-0.51***	0.45***	0.69***	0.67***	0.74***	0.30**	-0.12	-0.03	-0.29**
N			-0.19*	0.24	0.20*	0.01	-0.11	0.17	-0.16	-0.17	-0.22	-0.45***	-0.56***	0.39***	0.69***	0.64***	0.73***	0.25*	-0.11	-0.04	-0.27**
pH				0.16	-0.01	0.16	-0.22*	0.02	-0.36***	0.08	-0.41***	-0.28*	0.34**	0.24*	-0.07	0.04	-0.08	0.17	-0.23*	0.32***	-0.27**
Ah					0.31*	0.38**	-0.65***	0.34**	-0.40***	-0.04	-0.50***	-0.52***	0.00	0.41**	0.47**	0.52***	0.34*	0.42**	-0.23	0.08	-0.33*
Cover						0.49***	-0.61***	0.23*	-0.50***	0.06	-0.38**	-0.49***	0.16	0.26*	0.22	0.28*	0.30*	0.90***	0.01	0.09	-0.37***
Biomass							-0.50***	0.11	-0.39***	0.02	-0.47***	-0.33**	0.28*	0.13	0.10	0.23	0.12	0.48***	-0.09	0.13	-0.23*
Altitude								-0.13	0.72***	-0.05	0.68***	-0.25*	-0.37***	-0.33**	-0.35**	-0.33**	-0.64***	0.15	-0.28**	0.42***	0.42***
Aspect									0.00	-0.07	-0.04	-0.28*	-0.08	0.29*	0.04	0.16	0.15	0.23*	-0.10	-0.19	-0.16
Slope										-0.19*	0.76***	0.70***	-0.28*	-0.40***	-0.22*	-0.36**	-0.48***	-0.56***	0.22*	-0.37***	0.46***
Curv.											-0.19	0.05	0.34**	-0.14	-0.14	-0.16	-0.10	0.06	0.05	0.26	-0.03
cS												0.73***	-0.41***	-0.46***	-0.25*	-0.30**	-0.43***	-0.48***	0.30*	-0.46***	0.50***
mS													-0.08	-0.75***	-0.52***	-0.57***	-0.70***	-0.59***	0.32**	-0.25*	0.57***
fS														-0.16	-0.52***	-0.48***	-0.33**	0.16	-0.14	0.04	-0.13

Table 5 (continued)

	SOC	N	pH	Ah	Cover	Bio-mass	Altitude	Aspect	Slope	Curv.	eS	mS	fS	eSi	mSi	fSi	Cl	C3_cov	C4_cov	Spec. No	C4/C3	
cSi															0.40***	0.46***	0.44***	0.39***	-0.23	0.20	-0.41***	
mSi															0.68***	0.67***	0.24	0.24	-0.08	0.13	-0.24	
fSi															0.71***	0.37**	0.15	0.37**	-0.11	0.15	-0.32*	
Cl																	0.43***	-0.30*	-0.01	-0.47***		
C3_cov																			-0.33***	0.16	-0.69***	
C4_cov																				-0.01	0.86***	
Spec. No																						-0.19

BD: bulk density; SOC: soil organic carbon concentration; N: total nitrogen concentration; Ah: thickness of Ah horizon; Curv.: curvature; cS: coarse sand; mS: medium sand; fS: fine sand; cSi: coarse silt; mSi: medium silt; fSi: fine silt; Cl: clay; C3_cov: C₃ plant cover; C4_cov: C₄ plant cover; Spec.No.: Number of plant species; C4/C3: proportion of C₄-to-C₃ plants
Level of significance: *: $p \leq 0.05$; **: $p \leq 0.01$; ***: $p \leq 0.001$

ratios and larger range values, indicating a more homogeneous spatial distribution of these parameters. Texture fractions showed also higher Nu/Si ratios in UG79 compared to other small grids. WDPT showed no distinct trend between grazing intensities. Large grids revealed low Nu/Si ratios for both texture fractions, pointing towards a relatively high degree of dependence of these parameters.

Maps of the most different grazing treatments UG79 and HG show the spatial pattern and spatial co-behaviour of WDPT, SOC, and two texture fractions (Fig. 2a, b). The spatial distribution of SOC in UG79 (Fig. 2a) clearly illustrates that areas with low SOC contents (central part of the map) were characterised by high wettability, confirming the negative correlation between SOC and WDPT (Table 4a). Other areas with high SOC contents corresponded well with high clay contents (e.g. north-western part of the maps). The spatial distribution of fine sand showed little agreement with the distribution of other presented parameters. In HG, the spatial distribution of the generally high wettability corresponded well with the distribution of fine sand and clay. However, WDPT and SOC showed an opposite behaviour compared to UG79.

Large-scale variability particularly reflected topographical effects of the undulating landscape. As shown for CG_{large} in Fig. 3, the thickness of the Ah horizon was found to be very variable, ranging from <20 cm on the erosion-prone hilltop to >1 m in the depression and leeward slope. For further consideration of erosion and deposition processes, we combined cS and mS to a mostly erosion-resistant, and fS and cSi to an erosion-sensitive texture fraction. In accordance with Table 5b, Fig. 3 illustrates opposite spatial gradients for fS+cSi compared to cS+mS, resulting in a decreasing proportion of coarse material from up to 20–25% at the hilltop to less than 5% in the depression, whereas finer texture fractions raise by 15% with decreasing altitude. This clearly illustrates the topography-dependent sorting of particle size fractions in the landscape.

General linear model approach to evaluate impacts of topography and grazing

Cluster analysis resulted in four altitude classes, four aspect classes, three slope classes and five curvature

Table 6 Semivariogram parameters of selected topsoil properties (nugget (Nu), sill (Si) and range values, all derived from spherical models)

a)		Nu (Co)	Si (Co+Cs)	Nu/Si	Range (m)		Nu (Co)	Si (Co+Cs)	Nu/Si	Range (m)
UG79	fS	2.1083	8.4750	0.25	164	UG99	2.0000	40.000	0.05	85
	Clay	0.8000	3.8000	0.17	135		0.2000	6.5000	0.03	80
	WDPT	193.15	419.25	0.46	113		48.189	304.40	0.16	140
	BD ^a	0.0050	0.0093	0.54	41		0.0045	0.0158	0.29	80
	SOC ^a	14.30	31.20	0.46	60		5.60	46.10	0.12	80
CG	fS	1.8919	22.938	0.08	140	HG	1.1500	14.174	0.08	146
	Clay	0.0000	10.451	0.00	230		0.3020	3.9609	0.08	68
	WDPT	6.9511	7.0784	0.98	22		1.1642	1.4546	0.80	95
	BD ^a	0.0004	0.0035	0.11	70		0.0010	0.0067	0.15	47
	SOC ^a	3.50	10.50	0.33	85		4.10	20.0	0.20	82
WG _{large}	cS+mS	1.2326	12.884	0.10	253	CG _{large}	6.890	33.50	0.21	278
	fS+cSi	5.6329	18.760	0.30	212		5.690	19.84	0.29	89
	Ah	0.043	0.086	0.50	132		0.063	0.143	0.44	390

^aData from Steffens et al. 2009a

classes (Table 7). GLM was calculated for all topsoil and vegetation variables using these topographical classes. The models with the highest explained variance were shown in Table 8a. R squared values ranged between 41% for SOC stocks and 69% for Ah thickness and cS+mS; adjusted R squared values ranged from 23% for SOC stocks to 57% for cS+mS. Main effects and interactions between two and three factors were displayed, whereas higher order effects were excluded because no significant effects were found. Generally, texture classes were well explained by topography classes. Curvature alone had no significant influence on any of the analysed variables. Altitude was identified as most important factor for most variables (Table 8a).

Entering grazing treatment as additional influencing factor into GLM resulted in higher explained variance for WDPT and SOC stocks (R squared >50%; adjusted R squared >30%), and highest R squared values between 65 and 78% for Ah, biomass and texture classes (Table 8b). Biomass showed highest increase of explained variance from 32% to 72% after considering grazing classes. Grazing contributed strongly to the explained variance for each variable. Biomass and SOC stocks were nearly exclusively explained by the factor grazing, whereas topographic factors are less relevant.

Discussion

Distribution of topsoil and vegetation parameters on the scale of a landscape section

Impact of topography

Throughout all grazing intensities, topsoil texture was dominated by fine sand (34–54%) and coarse silt (14–24%; Tables 2 and 3), known to be the particle sizes mostly prone to wind erosion (Iversen and White 1982; Shao and Lu 2000; Hoffmann et al. 2008c). In addition, 75–83% of the soil material were present in particles and aggregates with a size <630 μm (Table 1), indicating a low degree of macro-aggregation. These results point towards wind erosion and deposition as important processes affecting the spatial distribution of topsoil properties on the landscape scale. In this context, correlations between topographic parameters (altitude and slope angle) and soil texture (Table 5) emphasised the sorting of particle size fractions in the landscape. Hilltops and steep slopes were characterised by up to 20% higher proportions of coarse particles (cS+mS), indicating a selective loss as well as less deposition of fine mineral fractions by wind erosion. In contrast, the proportion of finer particles (fS+cSi) increased with decreasing

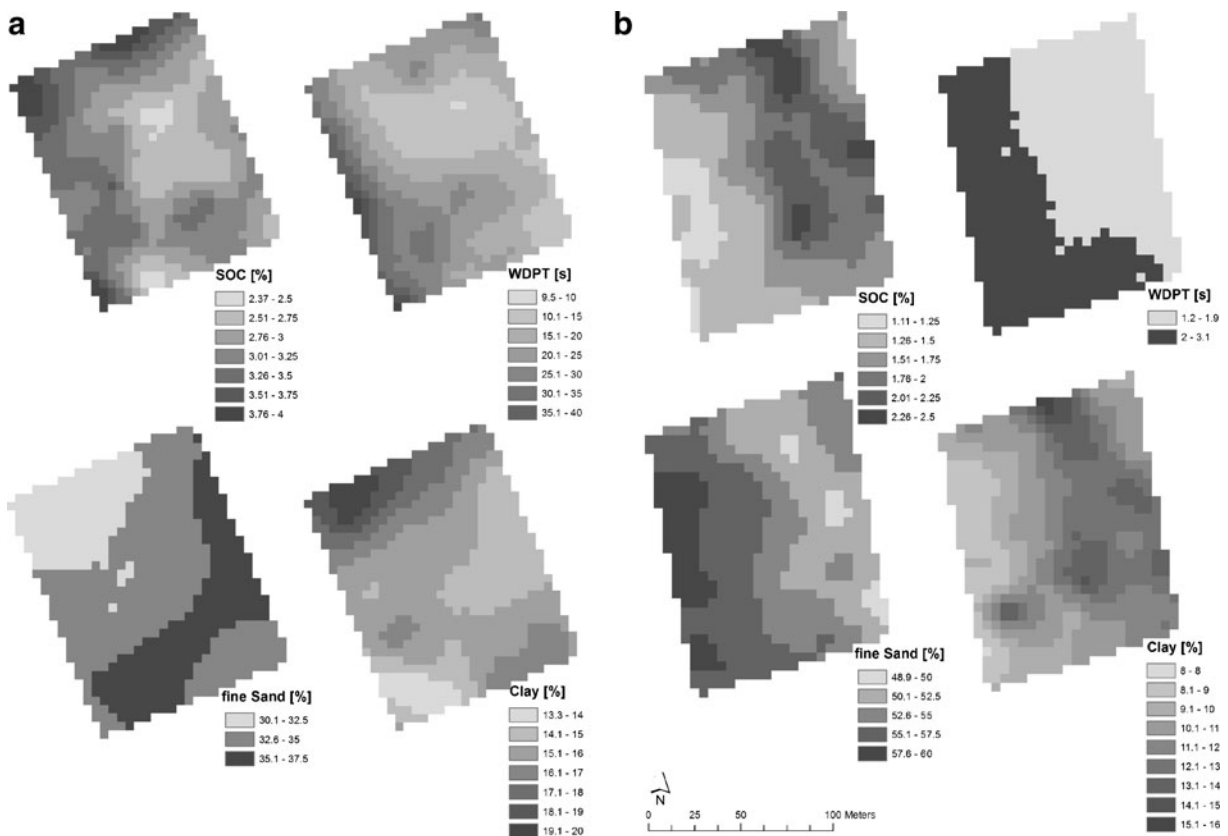


Fig. 2 a: Spatial distribution of soil organic carbon concentration (SOC), water drop penetration time (WDPT), proportion of fine sand and clay on UG 79. **b:** Spatial distribution of soil

organic carbon concentration (SOC), water drop penetration time (WDPT), proportion of fine sand and clay on HG

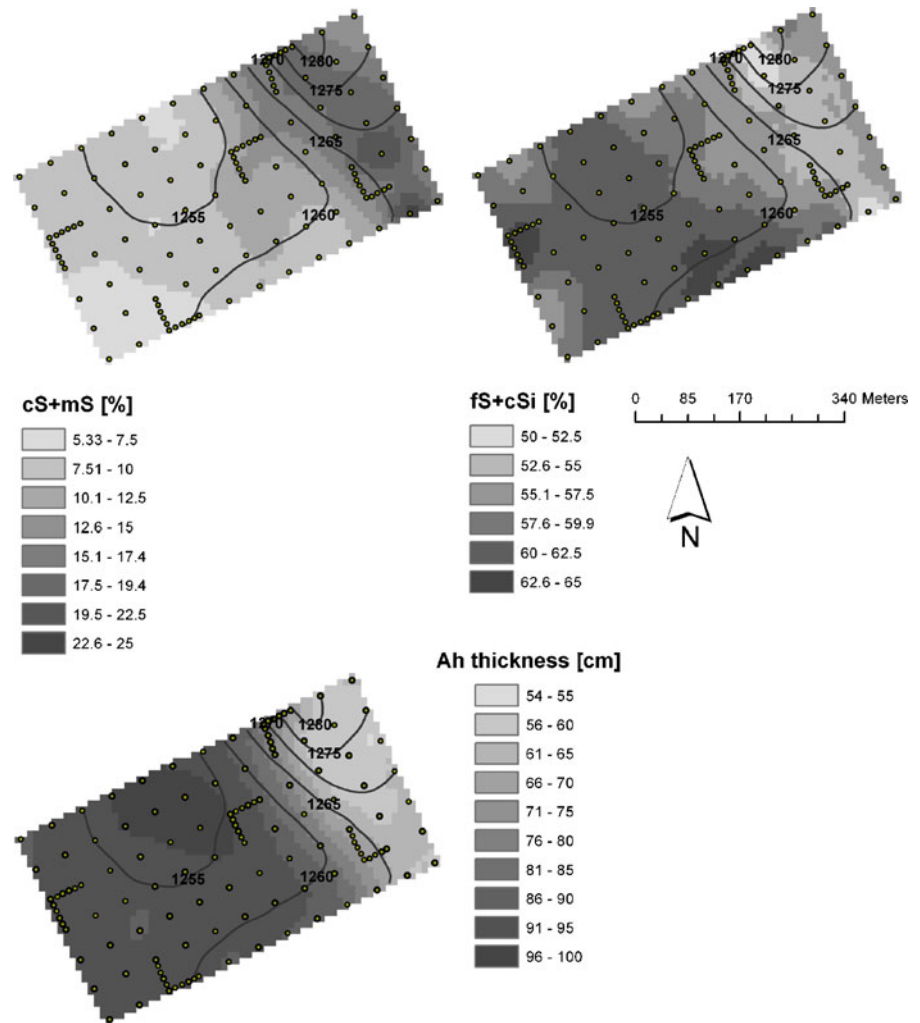
altitude and at less steep leeward slopes (Figs. 3 and 4). This is explained by lower wind speeds and associated higher dust deposition rates during frequent dust storms at leeward slopes compared to windward slopes and summits (Hoffmann et al. 2008a). In particular, steeper slope angles at windward exposed positions compared to leeward slopes can be related to the long-term effect of higher dust accumulation at leeward positions.

This large-scale effect enabled us to explain the higher sand content of HG. Compared to the other plots, HG was situated further away in a plane area with little topographical wind protection, resulting in significantly lower proportions of silt and clay (Table 2). According to Hoffmann et al. (2008c), the average particle diameter of the total suspended dusts in the investigated area was 23 μm . This indicates a selective loss of fine particles due to wind erosion over a long period on HG. The other plots were situated at a leeward slope position, favouring

sedimentation of fine particles. This is confirmed by higher amounts of particles $<63 \mu\text{m}$ in all other plots compared to HG (Table 2).

More evidence for the spatial pattern of dust deposition can be drawn from the thickness of the Ah horizon, ranging from <20 cm on erosion-prone hilltops and windward slopes to >1 m in depressions and at leeward slopes (Fig. 3), emphasising the more protected situation of leeward slopes and depressions. As most of the generally low annual precipitation occurs during the vegetation period (May to September), water erosion can be neglected as reason for particle relocation in the investigated landscape section. However, Ah horizons were also largely influenced by the vegetation cover. Gili et al. (2010) found a significant interaction between vegetation patches and soil texture, and showed that water availability as determined by soil texture also affected the relative abundance of different herbaceous species. In our investigated area, north-oriented slopes

Fig. 3 Spatial distribution of thickness of Ah horizon, coarse sand + medium sand (cS+mS), and fine sand + coarse silt (fS+cSi) proportion of the large continuously grazed plot (CG_{large})



were characterised by higher aboveground biomass, higher species richness, higher average soil water contents and lower average soil temperatures, resulting in deeper Ah-horizons (Gong et al. 2008). Additionally, on both large plots altitude was negatively correlated with vegetation cover, and positively correlated with the ratio of C₄-to-C₃ plants (Table 5). C₄ species with their higher water use efficiency can be considered as indicators of dry habitats in this grassland ecosystem. Therefore, a higher abundance of C₄ plants on steeper slopes points towards lower water contents and less favourable growing conditions on slopes (Gong et al. 2008; Steffens et al. 2009a). Accordingly, multiple effects of topography were responsible for the spatial pattern of the topsoil thickness and species composition. On the one hand, erosion processes leave coarse soil particles behind,

leading to lower soil water contents, lower biomass production and shallower Ah horizons at exposed landscape positions. On the other hand, deposition of fine soil particles and higher soil water contents support higher biomass production and deeper Ah horizons at sheltered depressions. Topographic variability developed over pedogenic time scales and has therefore the largest effect on the distribution of long-lasting soil properties like stable SOC pools (Burke et al. 1999). As a consequence, topsoil parameters like SOC concentrations, $\delta^{13}\text{C}$ or pH values showed strong spatial correlations to topographic features (Steffens et al. 2009a). This clearly indicates that topography controls vegetation patterns as well as related variations in soil properties.

To conclude, the spatial distribution of soil texture in the landscape is mainly controlled by topography,

Table 7 Analysis of variance (F values) on topsoil and vegetation parameters based on GLM

	WDPT	SOC-stock	Ah	Biomass	cS+mS	fS+cSi
a: Results of GLM using topography clusters						
Corrected model	4.42***	2.32***	4.57***	2.77***	5.77***	4.31***
Intercept	127.95***	2656.52***	1835.06***	330.38***	1071.23***	17822.83***
Altitude	8.77***	1.34 NS	25.25***	1.30 NS	3.81**	2.14*
Aspect	2.14 NS	0.27 NS	2.42 NS	2.30 NS	14.76***	5.20**
Slope	1.83 NS	1.56 NS	1.81 NS	2.11 NS	2.40 NS	4.26**
Curvature	0.57 NS	0.60 NS	0.70 NS	0.40 NS	0.72 NS	0.65 NS
Altitude × Aspect	3.84**	1.41 NS	2.19*	3.37***	3.27***	0.76 NS
Altitude × Slope	5.22**	2.48*	3.76**	0.68 NS	1.14 NS	2.06*
Altitude × Curvature	3.05**	2.77**	1.98*	0.61 NS	2.01*	0.70 NS
Aspect × Slope	0.13 NS	1.12 NS	2.26*	0.67 NS	4.96***	1.88 NS
Aspect × Curvature	1.05 NS	0.80 NS	1.22 NS	0.51 NS	1.54 NS	2.35*
Slope × Curvature	2.72*	1.47 NS	0.84 NS	0.75 NS	3.18**	3.18**
Altitude × Aspect × Slope	1.10 NS	0.54 NS	0.90 NS	0.87 NS	3.41**	3.58**
Altitude × Aspect × Curv.	3.35**	0.78 NS	1.35 NS	1.17 NS	4.68***	2.08*
Altitude × Slope × Curv.	1.24 NS	1.17 NS	1.16 NS	0.83 NS	7.21***	4.38***
Aspect × Slope × Curv.	1.24 NS	2.01*	0.15 NS	0.50 NS	1.36 NS	0.80 NS
R Squared	0.52	0.41	0.69	0.50	0.69	0.63
Adjusted R squared	0.40	0.23	0.54	0.32	0.57	0.48
b: Results of GLM using topography clusters and grazing intensities						
Corrected model	4.40***	2.57***	5.66***	8.24***	10.13***	5.90***
Intercept	146.64***	3550.02***	3563.48***	1174.84***	2324.87***	31769.40***
Altitude	7.04***	0.55 NS	20.71***	4.08**	34.71***	11.35***
Aspect	1.17 NS	0.46 NS	4.95**	0.06 NS	12.53***	4.30**
Slope	2.51 NS	1.72 NS	0.40 NS	0.95 NS	1.00 NS	0.54 NS
Curvature	0.31 NS	0.90 NS	1.02 NS	1.00 NS	1.00 NS	0.40 NS
Grazing	4.34*	8.35***	4.56**	52.23***	7.25***	10.58***
Altitude × Aspect	7.82***	0.39 NS	2.10 NS	0.50 NS	3.38**	3.85**
Altitude × Slope	6.27*	0.68 NS	3.97**	0.62 NS	18.27***	6.69**
Altitude × Curvature	4.38***	0.91 NS	1.77 NS	1.10 NS	1.78 NS	1.60 NS
Altitude × Grazing	.	0.89 NS	1.12 NS	0.09 NS	1.09 NS	0.36 NS
Aspect × Slope	0.09 NS	0.78 NS	0.68 NS	0.63 NS	1.55 NS	1.41 NS
Aspect × Curvature	1.24 NS	0.43 NS	1.23 NS	0.51 NS	2.20*	0.78 NS
Aspect × Grazing	0.01 NS	0.41 NS	0.90 NS	0.44 NS	0.95 NS	1.19 NS
Slope × Curvature	2.65*	0.85 NS	1.00 NS	0.58 NS	2.79*	3.42**
Slope × Grazing	.	0.13 NS	0.60 NS	0.37 NS	1.16 NS	0.20 NS
Curvature × Grazing	0.08 NS	0.80 NS	0.94 NS	1.08 NS	2.54**	0.89 NS
R squared	0.54	0.54	0.81	0.82	0.86	0.79
Adjusted R squared	0.42	0.33	0.67	0.72	0.78	0.65

Level of significance: *: $p \leq 0.05$; **: $p \leq 0.01$; ***: $p \leq 0.001$

Table 8 Mean values of topsoil parameters of respective topographic clusters

	Cluster	Mean	Std. Dev.	<i>n</i>	<i>n</i> in %	WDPT	SOC-stock	Ah	Biomass	cS+mS	fS+cSi		
Altitude (m)	1	1,257	1.40	217	40.9	10.5	c 1.002	c 95.0	a 244.5	a 9.2	c 61.2	a	
	2	1,261	1.35	67	12.6	28.0	a 1.142	a 83.0	b 243.8	a 14.3	a 56.6	b	
	3	1,269	2.26	88	16.6	15.1	bc 1.035	bc 72.1	c 244.3	a 11.2	b 57.9	b	
	4	1,276	2.49	158	29.8	15.9	b 1.050	b 64.8	d 268.8	a 12.4	b 57.0	b	
Aspect (°)	1	325	22	NW	226	42.6	14.2	b 1.045	b 79.0	b 283.0	a 9.6	c 59.6	b
	2	225	23	SW	68	12.8	6.5	b 1.055	b 71.0	c 141.9	c 14.9	a 55.3	d
	3	20	14	NNE	98	18.5	21.9	a 1.135	a 80.4	b 285.7	a 11.7	b 57.5	c
	4	87	26	E	138	26.0	9.6	b 0.955	c 88.9	a 219.3	b 9.7	c 61.6	a
Slope (%)	1	13.5	2.7		46	8.7	34.0	a 1.072	a 63.0	c 159.2	b 14.1	a 55.0	c
	2	6.9	1.6		184	34.7	15.8	a 1.085	a 74.5	b 254.3	a 11.4	b 57.9	b
	3	3.0	1.1		300	56.6	14.0	a 1.006	b 88.2	a 271.7	a 9.8	c 60.7	a
Curvature (rad m ⁻¹)	1	1.21	0.25	Convex	14	2.6	28.9	a 1.160	a 51.3	c 287.6	a 11.3	a 54.5	b
	2	0.42	0.15		60	11.3	17.2	b 1.062	ab 72.2	b 244.1	ab 11.4	a 58.3	a
	3	0.09	0.07		224	42.3	14.8	b 1.027	b 82.5	a 271.7	ab 11.0	a 59.9	a
	4	-0.13	0.09		190	35.8	12.6	b 1.029	b 83.9	a 241.1	ab 10.1	a 59.3	a
	5	-0.51	0.22	Concave	42	7.9	13.2	b 1.078	ab 80.3	a 211.0	b 11.2	a 58.7	a
Grazing	1			WG _{large}	122	23.0	.	1.121	b 64.4	d 167.3	c 10.2	b 56.8	d
	2			CG _{large}	123	23.2	.	1.064	c 81.8	bc 162.7	c 11.8	b 58.3	c
	3			UG99	99	18.7	15.6	b 0.962	d 77.1	c 405.4	a 10.7	b 60.1	b
	4			UG79	98	18.5	21.6	a 1.168	a 86.0	b 310.8	b 15.3	a 55.4	d
	5			CG	88	16.6	5.8	c 0.836	e 97.8	a .	7.7	c 63.4	a

Different letters indicate that the mean difference is significant at the 0.05 level

affecting erosion and deposition processes. Consequences are different conditions for plant growth, shifts in the plant community, and low development of Ah horizons at hilltops and steep slopes.

Discrimination between topography- and grazing-related effects

Geostatistics highlighted the effects of topography on particle relocation processes. However, different grazing intensities may noticeably interfere with topography-related topsoil properties (Fig. 4a, b). All grazed sites showed a low dust emission flux caused by local erosion, while ungrazed sites were well protected against wind erosion and acted as dust sinks (Hoffmann et al. 2008a, b). This effect most likely amplifies the spatial pattern of topsoil properties, which are basically caused by the topography.

To differentiate between the effects of grazing treatments and the effects of topography (wind

erosion and deposition processes), a multifactorial approach was applied. A GLM considering topographic features (Table 8a) identified aspect as the most important factor. Multiple (3-fold) interactions between topographical features were most important for the explanation of the erosion-pointing texture fractions: cS+mS and fS+cSi. WDPT and Ah were less, and SOC stock and biomass least influenced by topography. This is in contrast to Sigua and Coleman (2010), who found a strong influence of aspect and slope position on SOC concentration in subtropical pastures, and explained more than 70% of SOC's spatial variability by differences in soil texture (clay content). In our case, other factors were more important for the explanation of SOC parameters. Grazing had a highly significant impact on all variables when it was included in the models (Table 8b). Strongest effects were found on above-ground biomass, as it was exclusively explained by grazing. Similar to aboveground biomass, also SOC

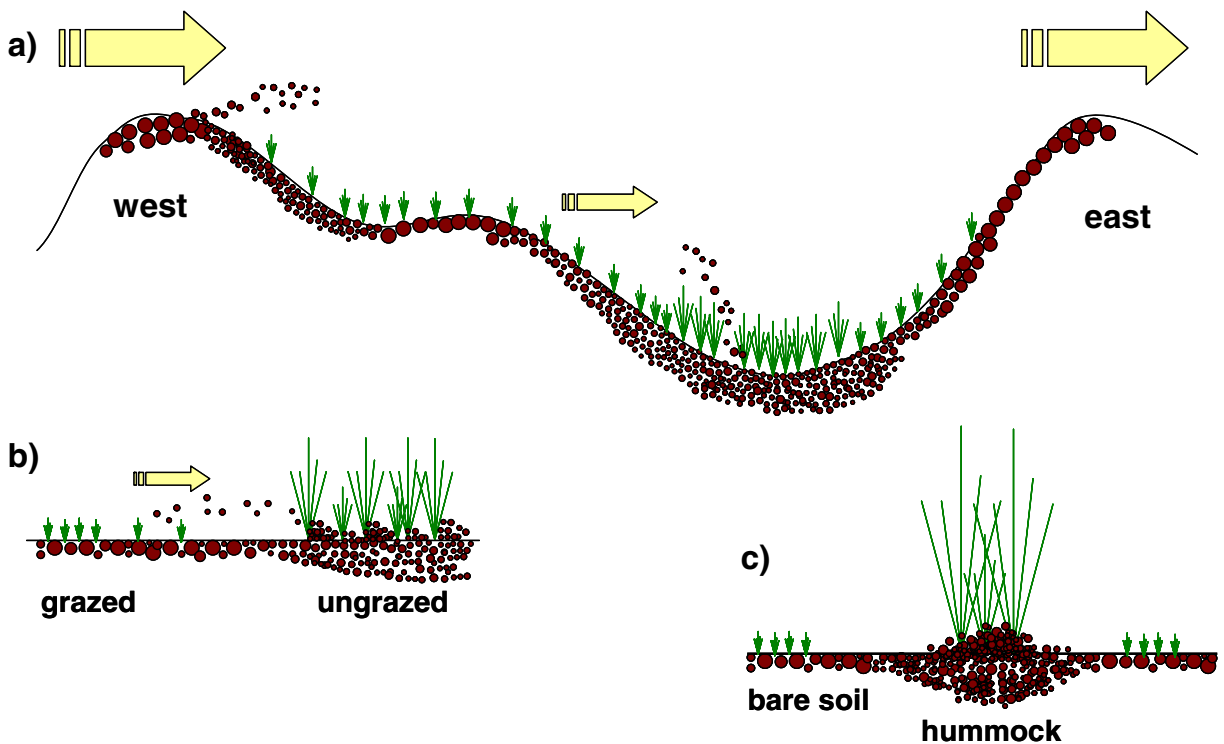


Fig. 4 Development of spatial variability of topsoil parameters (texture and thickness of Ah horizon) in steppe region. This conceptual model includes a landscape section (a), plot scale

(b), and pit scale (c). Figure 4c is on the basis of Burke et al. (1999), modified

stocks were exclusively explained by grazing, most likely due to the fact that biomass production directly influences topsoil SOC stocks.

Texture and Ah were well explained by both, topography and grazing. While topography led to a sorting of particle size fractions in the landscape, grazing altered the deposition of fine particles indirectly via aboveground biomass and roughness lengths (Hoffmann et al. 2008a, b). Both led to different Ah-thicknesses in the investigated area. There were only weak effects of grazing on WDPT; this parameter was best explained by altitude-related topography features.

To conclude, the GLM identified grazing as the factor with the highest impact on biomass-related soil properties, whereas texture was mainly influenced by both: grazing and topography. This indicates that intensive grazing and grazing exclusions can amplify the spatial pattern of topsoil parameters. The GLM procedures allowed to quantify the influence of different factors, but geostatistical evaluations are still

needed to obtain information on spatial distribution and spatial interactions within differently grazed plots.

Grazing-induced spatial pattern on the plot scale

Comparing small grids, grazing intensity was reflected strongly in the vegetation parameters, mainly aboveground biomass (Table 2) that is known to affect wind erosion and deposition processes (Hoffmann et al. 2008a, b). However, the texture fractions showed no relation to grazing treatments at the plot scale (Table 2). Other topsoil properties showed obvious trends from ungrazed to grazed sites, as reflected by e.g. lower WDPT, SOC and N values and higher bulk densities. Regarding the spatial dependence within small grids, UG79 had higher Nu/Si ratios for the analysed topsoil parameters when compared to the other treatments (Table 6). For the texture fractions, this was accompanied by large range values, indicating that their spatial pattern was controlled by processes on larger scales. For BD and

SOC, this was accompanied by small range values, indicating a more heterogeneous, patchy distribution of these parameters in the long-term ungrazed plot. We attribute the heterogeneity of BD and SOC to the scattering effects of recovering soil structure and advancing succession of vegetation without grazing stress, which can be ascribed to self-organising processes occurring in arid ecotons (Bestelmeyer et al. 2006). The established mosaic of vegetation cover (Steffens et al. 2009a) leads to spatially variable litter inputs. The resultant increase of POM contents (Table 1 and Steffens et al. 2009b) leads not only to high SOC contents, but also to a high spatial variability of SOC in UG79. More evidence can be drawn from Wiesmeier et al. (2009), who clearly showed that the increase of SOC after grazing exclusion is spatially restricted to vegetation patches and from Burke et al. (1999) who showed that resource islands (hummocks) form around grass tussocks and shrubs. The more patchy or heterogeneous pattern of SOC displays the formation of resource patches under grass tussocks after grazing exclusion (Fig. 4c and Wiesmeier et al. 2009). In contrast, intensive grazing leads to a modification of topsoil properties and their spatial distribution. Especially under semi-arid climatic conditions, consumption of biomass by sheep and hoof action removed vegetation patches and led to a homogenisation of chemical and physical soil properties (Steffens et al. 2009a; Wiesmeier et al. 2009).

The spatial distribution of SOC at UG79 clearly indicated that areas with low concentrations also showed high wettability values (measured as WDPT; Fig. 2a). We assume the reduced water repellency to be a consequence of the lower amount of topsoil SOC. These observations were supported by a significantly positive correlation between WDPT and SOC within UG79 (Table 4a), indicating that the organic substance reduced the rate of wetting (Zhao et al. 2007). It is remarkable that HG showed generally high wettability values, too. The spatial distribution of WDPT in HG corresponded well with the distribution of fine sand and clay and showed strong correlations between soil hydraulic parameters and texture fractions (Table 4d). However, WDPT and SOC showed an opposite behaviour compared to UG79. At SOC-rich and well-structured sites SOC controls the WDPT, while texture is determinative on sites with depleted SOC

and a more coherent or homogenized soil structure. Beside WDPT, also K is texture-controlled in SOC-depleted grazed and therefore most often homogenized grassland topsoils (Table 4d).

In addition to positive correlations between WDPT and SOC, both ungrazed plots showed positive correlations between vegetation cover and thickness of Ah (Table 4a, b). This supports the assumption that grazing exclusion promotes plant growth, dust deposition and the development of an SOC-rich Ah horizon, which in turn influences the hydraulic properties in ungrazed steppe topsoils.

To conclude, grazing intensified the topography-controlled soil texture distribution, and strongly altered SOC amounts and distributions as well as soil hydraulic functions. On the plot scale, we were able to identify WDPT-SOC interactions on grazing exclosures and WDPT-texture interactions on heavily grazed plots. Spatial homogenisation of topsoil parameters due to grazing was also detected on the plot scale and points to the high vulnerability of topsoils, due to the low structural stability of these steppe soils.

Grazing-induced alterations of topsoil properties on the pit scale

Investigations on the pit scale (square meter) revealed more detailed information of grazing impacts on topsoils. Higher bulk densities within the grazed plots (Table 2) were accompanied by a lower angle of internal friction, indicating a lower degree of aggregation. Not only higher cohesion values, but also lower hydraulic conductivities underline this more compressed situation of the grazed topsoils (Table 1, Krümmelbein et al. 2006). Higher bulk densities at places with high grazing pressure are most likely the result of three different but related effects: (a) homogenisation and compaction due to animal trampling result in (b) lower mechanical soil stability (Krümmelbein 2007), and is further enhanced by (c) lower contents of SOC (Steffens et al. 2008). Lower SOC concentrations and SOC stocks are mainly explained by lower proportions of both free and aggregate-occluded POM (Table 1). In the ungrazed areas, the amount of aggregate-occluded POM was twice the amount in the grazed plots proving the formation of stronger aggregates compared to grazed topsoils. This was also supported by the greater

angles of internal friction in the ungrazed compared to the grazed sites (Krümmelbein et al. 2006).

Higher amounts of POM in ungrazed compared to grazed plots can be explained by higher aboveground biomass and vegetation cover, leading to higher litter inputs. More evidence can be drawn from the total belowground biomass, as it also increases significantly with decreasing grazing intensity and corresponds well to the higher SOC contents at ungrazed sites (Gao et al. 2008). Additionally, grazing may lead to enhanced POM decomposition following aggregate deterioration due to trampling (Steffens et al. 2008). This becomes clearly obvious in incubation experiments with optimised conditions for decomposition processes. Due to the low physical protection of POM and SOC in less structured topsoils of the grazed sites, it is readily available for mineralisation. Therefore, lower amounts of SOC and POM at the grazed sites are in line with much higher SOC mineralisation compared to ungrazed sites (Table 1). Under field conditions, input of SOC from trampling and thorough mixing of the topsoil by hoof action is known to result in a highly active soil biotic community, which rapidly turns over SOC (Beukes and Cowling 2003). Although the quantity of SOC is higher at ungrazed sites, the protection in form of aggregate-occlusion reduces the accessibility of SOC for microbes and thus hinders its mineralisation. Similar to higher WDPT values in ungrazed plots (Table 2), Reszkowska et al. (2010) found higher contact angles, i.e. higher water repellencies at UG79 compared to the grazed sites, underlining the reduced accessibility of SOC for microbes on the pit scale. This leads to the consideration of significant correlations between SOC contents and hydraulic soil properties. These interactions were already mentioned for the plot scale, but were also identified and explained at the pit scale. WDPT was higher in ungrazed than in grazed plots, with highest values in UG79 (Table 2; Zhao et al. 2007). UG79 had the highest SOC concentrations and lowest bulk densities, being most likely responsible for the low wettability of this material. This is in line with Goebel et al. (2005) who considered SOC to be the main source of hydrophobicity and explained large contact angles of grassland topsoils by large SOC contents. Steffens et al. (2009b) found SOC quality (^{13}C CPMAS-NMR spectroscopy, neutral sugar analytics) to be similar between different grazing intensities. Therefore, the quantity of POM is most likely the key

driver for the observed strong water repellency values in the grazing enclosures and not POM quality. In turn, the reduced wettability enhances the stability of aggregates (Goebel et al. 2005), which stabilises encapsulated SOC by physical separation, indicating a self-supporting process.

To conclude, on the square meter scale the amount of POM and the functioning of soil structure down to a μm -scale react most sensitively to grazing and are identified as key-drivers for SOC balances and hydraulic soil functions on plot and landscape scales.

Conclusions

Interdisciplinary multi-scale investigations of topsoil and vegetation properties and of topographic features are necessary to understand the intertwined processes that occur in intensively grazed steppe areas. The present study compared grazing-topsoil and grazing-vegetation interactions on different spatial scales, and distinguishes between topography and grazing as main influencing factors for the spatial distribution of these parameters in the landscape.

On the scale of a landscape section, *topography* controlled the soil texture distribution, due to long term erosion and deposition processes. *Grazing* had strongest effects on the aboveground biomass production and biomass-related topsoil-SOC. Ah was influenced by both, biomass input due to grazing and particle relocation due to topography. Therefore, the heterogeneous topography led to differences in Ah-thickness throughout the landscape and consequently a differentiated distribution of topsoil characteristics. Grazing intensity interfered with the topography-controlled soil texture distribution, and strongly altered SOC amounts and distributions and—less pronounced—soil hydraulic functions. On the plot scale, we were able to identify wettability-SOC interactions on grazing enclosures and wettability-texture interactions on heavily grazed plots.

On the soil pit scale, relevant processes behind the grazing-induced changes of topsoil properties were identified. Intensive grazing of sensitive steppe topsoils led to a strong reduction of aboveground biomass and litter input, resulting in lower SOC and especially POM amounts. Lower SOC protection due to reduced aggregation in combination with animal trampling led to an enhanced mineralisation of SOC

in grazed areas. This was accompanied by higher topsoil bulk densities, lower infiltration rates, and subsequently a higher risk of soil erosion, especially by wind. Topsoils of grazing exclosures were characterised by higher POM contents, mechanically more stable conditions and a negligible risk of soil erosion.

Acknowledgements The authors thank the Deutsche Forschungsgemeinschaft for the funding of the Research Unit 536 MAGIM (Matter fluxes in grasslands of Inner Mongolia). Xingguo Han and the Institute of Botany are gratefully acknowledged for giving us the opportunity to work at IMGERS. We thank Xiaoying Gong for providing additional information on site characteristics of different slope positions. We also thank both anonymous reviewers for their suggestions. The detailed comments were very helpful to improve the manuscript.

References

- Bestelmeyer BT, Ward JP, Havstad KM (2006) Soil-geomorphic heterogeneity governs patchy vegetation dynamics at an arid ecotone. *Ecology* 87:963–973
- Beukes PC, Cowling RM (2003) Non-selective grazing impacts on soil-properties of the Nama Karoo. *J Range Manage* 56:547–552
- Burke IC, Lauenroth WK, Riggle R, Brannen P, Madigan B, Beard S (1999) Spatial variability of soil properties in the shortgrass steppe: the relative importance of topography, grazing, microsite, and plant species in controlling spatial patterns. *Ecosystems* 2:422–438
- Buyanovsky GA, Aslam M, Wagner GH (1994) Carbon turnover in soil physical fractions. *Soil Sci Soc Am J* 58:1167–1173
- Cambardella CA, Moorman TB, Parkin TB, Karlen DL (1994) Field-scale variability of soil properties in central Iowa soils. *Soil Sci Soc Am J* 58:1501–1511
- Conant RT, Paustian K, Elliott ET (2001) Grassland management and conversion into grassland: effects on soil carbon. *Ecol Appl* 11:343–355
- Cui XY, Wang YF, Niu HS, Wu J, Wang SP, Schnug E, Rogasik J, Fleckenstein J, Tang YH (2005) Effect of long-term grazing on soil organic carbon content in semiarid steppes in Inner Mongolia. *Ecol Res* 20:519–527
- Dormaar JF, Willms WD (1998) Effect of forty-four years of grazing on fescue grassland soils. *J Range Manage* 51:122–126
- Dubeux JCB, Sollenberger LE, Comerford NB, Scholberg JM, Ruggieri AC, Vendramini JMB, Interrante SM, Portier KM (2006) Management intensity affects density fractions of soil organic matter from grazed bahiagrass swards. *Soil Biol Biochem* 38:2705–2711
- Ellert BH, Bettany JR (1995) Calculation of organic matter and nutrients stored in soils under contrasting management regimes. *Can J Soil Sci* 75:529–538
- Gao YZ, Giese M, Lin S, Sattelmacher B, Zhao Y, Brück H (2008) Belowground net primary productivity and biomass allocation of a grassland in Inner Mongolia is affected by grazing intensity. *Plant Soil* 307:41–50
- Gao YZ, Giese M, Han WDL, Zhou ZY, Brück H, Lin S, Taube F (2009) Land use and drought interactively affect interspecific competition and species diversity at the local scale in a semiarid steppe ecosystem. *Ecol Res* 24:627–635
- Giese M, Gao YZ, Zhao Y, Pan Q, Lin S, Peth S, Brück H (2009) Effects of grazing and rainfall variability on root and shoot decomposition in a semi-arid grassland. *Appl Soil Ecol* 41:8–18
- Gili AA, Trucco R, Niveyro S, Balzarini M, Estelrich D, Quiroga A, Noellemeyer E (2010) Soil texture and carbon dynamics in savannah vegetation patches of central Argentina. *Soil Sci Soc Am J* 74:647–657
- Goebel MO, Bachmann J, Woche SK, Fischer WR (2005) Soil wettability, aggregate stability, and the decomposition of soil organic matter. *Geoderma* 128:80–93
- Gong X, Brück H, Giese KM, Zhang L, Sattelmacher B, Lin S (2008) Slope aspect has effects on productivity and species composition of hilly grassland in the Xilin River Basin, Inner Mongolia, China. *J Arid Environ* 72:483–493
- Hartge KH, Horn R (2009) Die physikalische Untersuchung von Böden [Measuring the physical parameters of soils: methods, application, and assessment.] 4. Aufl. Schweizerbart'sche Verlagsbuchhandlung, Science Publishers, Stuttgart
- Heinemeyer O, Insam H, Kaiser EA, Walenzik G (1989) Soil microbial biomass and respiration measurements: an automated technique based on infra-red gas analysis. *Plant Soil* 116:191–195
- Hoffmann C, Funk R, Wieland R, Li Y, Sommer M (2008a) Effects of grazing and topography on dust flux and deposition in the Xilingele grassland, Inner Mongolia. *J Arid Environ* 72:792–807
- Hoffmann C, Funk R, Li Y, Sommer M (2008b) Effect of grazing on wind driven carbon and nitrogen ratios in the grasslands of Inner Mongolia. *Catena* 75:182–190
- Hoffmann C, Funk R, Sommer M, Li Y (2008c) Temporal variations in PM₁₀ and particle size distribution during Asian dust storms in Inner Mongolia. *Atmos Environ* 42:8422–8431
- IUSS Working Group WRB (2006) World reference base for soil resources 2006. World Soil Resources Reports, 103. FAO, Rome
- Iversen JD, White BR (1982) Saltation threshold on Earth, Mars and Venus. *Sedimentology* 29:111–119
- Jastrow JD, Amonette JE, Bailey VL (2007) Mechanisms controlling soil carbon turnover and their potential application for enhancing carbon sequestration. *Clim Change* 80:5–23
- Kölbl A, von Lütow M, Kögel-Knabner I (2006) Decomposition and distribution of ¹⁵N labelled mustard litter (*Sinapis alba*) in physical soil fractions of a cropland with high- and low-yield field areas. *Soil Biol Biochem* 38:3292–3302
- Kölbl A, von Lütow M, Rumpel C, Munch JC, Kögel-Knabner I (2007) Dynamics of ¹³C-labeled mustard litter (*Sinapis alba*) in particle-size and aggregate fractions in an agricultural cropland with high- and low-yield areas. *J Plant Nutr Soil Sci* 170:123–133

- Krümmlbein J (2007) Influence of various grazing intensities on soil stability and water balance of grassland soils in Inner Mongolia, P. R. China. Schriftenreihe Institut für Pflanzenernährung und Bodenkunde, Universität Kiel, Nr. 74. Hrsg. R. Horn und K.H. Mühling, 85pp., ISSN 0933-68074
- Krümmlbein J, Wang Z, Zhao Y, Peth S, Horn R (2006) Influence of various grazing intensities on soil stability, soil structure and water balance of grassland soils in Inner Mongolia. P R China Adv Geocol 38:93–101
- Krümmlbein J, Peth S, Horn R (2008) Determination of pre-compression stress of a variously grazed steppe soil under static and cyclic loading. Soil Tillage Res 99:139–148
- Müller C (2009) Carbon sequestration and soil organic matter composition affected by altered soil aggregate dynamics due to land-use changes. Dissertation, Technische Universität München
- Noellemeyer E, Quiroga AR, Estelrich D (2006) Soil quality in three range soils of the semi-arid Pampa of Argentina. J Arid Environ 65:142–155
- Pebesma EJ (2004) Multivariable geostatistics in R: the gstat package. Comput Geosci 30:683–691
- Proffitt APB, Jarvis RJ, Bendotti S (1995) The impact of sheep trampling and stocking rate on the physical properties of a Red Duplex Soil with two initially different structures. Aust J Agric Res 46:733–747
- Quiroga AR, Buschiazzi DE, Peinemann N (1998) Management discriminant properties in semi-arid soils. Soil Sci 163:591–597
- RDevelopmentCoreTeam (2008) R: a language and environment for statistical computing. R Foundation for Statistical Computing, Vienna, Austria
- Reszkowska A, Peth S, Krümmlbein J, Zhao Y, Kölbl A, Horn R (2010) Effect of land use management on changes in physical properties from the aggregate to the landscape scale. Soil Till Res submitted
- Shao Y, Lu H (2000) A simple expression for wind erosion threshold friction velocity. J Geophys Res 105:22437–22443
- Sigua GC, Coleman SW (2010) Spatial distribution of soil carbon in pastures with cow-calf operation: effects of slope aspect and slope position. J Soils Sediments 10:240–247
- Soussana JF, Loiseau P, Vuichard N, Ceschia E, Balesdent J, Chevallier T, Arrouays D (2004) Carbon cycling and sequestration opportunities in temperate grasslands. Soil Use Manage 20:219–230
- Steffens M, Kölbl A, Totsche KU, Kögel-Knabner I (2008) Grazing effects on soil chemical and physical properties in a semiarid steppe of Inner Mongolia (P.R. China). Geoderma 143:63–72
- Steffens M, Kölbl A, Giese M, Hoffmann C, Totsche KU, Breuer L, Kögel-Knabner I (2009a) Spatial variability of topsoils and vegetation in a grazed steppe ecosystem in Inner Mongolia (P.R. China). J Plant Nutr Soil Sci 172:78–90
- Steffens M, Kölbl A, Kögel-Knabner I (2009b) Alteration of soil organic matter pools and aggregation in semi-arid steppe topsoils as driven by organic matter input. Eur J Soil Sci 60:198–212
- Veldkamp E (1994) Organic-carbon turnover in 3 tropical soils under pasture after deforestation. Soil Sci Soc Am J 58:175–180
- von Lütow M, Kögel-Knabner I, Ekschmitt K, Matzner E, Guggenberger G, Marschner B, Flessa H (2006) Stabilization of organic matter in temperate soils: mechanisms and their relevance under different soil conditions—a review. Eur J Soil Sci 57:426–445
- Wiesmeier M, Steffens M, Kölbl A, Kögel-Knabner I (2009) Degradation and small-scale spatial homogenization of topsoils in intensively-grazed steppes of Northern China. Soil Tillage Res 104:299–310
- Wu HB, Guo ZT, Peng CH (2003) Land use induced changes of organic carbon storage in soils of China. Glob Chang Biol 9:305–315
- Zhao Y, Peth S, Krümmlbein J, Horn R, Wang ZY, Steffens M, Hoffmann C, Peng XH (2007) Spatial variability of soil properties affected by grazing intensity in Inner Mongolia grassland. Ecol Model 205:241–254